TISSUE ENGINEERING: Part A
Volume 00, Number 00, 2010

DOI: 10.1089/ten.tea.2009.0589

Original Article

Viable Fibroblast Matrix Patch Induces Angiogenesis and Increases Myocardial Blood Flow in Heart Failure After Myocardial Infarction

Jordan Lancaster, B.S.,[1] Elizabeth Juneman, M.D.,[1] Tracy Hagerty, M.D.,[1] Rose Do, M.D.,[1] Michael Hicks, B.S.,[2] Kate Meltzer, M.S.,[3] Paul Standley, Ph.D.,[3] Mohamed Gaballa, Ph.D.,[4] Robert Kellar, Ph.D.,[5] Steven Goldman, M.D.,[1] and Hoang Thai, M.D.[1]

Background: This study examines a viable biodegradable three-dimensional fibroblast construct (3DFC) in a model of chronic heart failure. The viable fibroblasts, cultured on a vicryl mesh, secrete growth factors that stimulate angiogenesis.
Methods: We ligated the left coronary artery of male Sprague-Dawley rats, implanted the 3DFC 3 weeks after myocardial infarction and obtained end point data 3 weeks later, that is, 6 weeks after myocardial infarction.
Results: Implanting the 3DFC increases ($p < 0.05$) myocardial blood flow twofold, microvessel formation (0.02 ± 0.01 vs. 0.07 ± 0.03 vessels/μm^2), and ventricular wall thickness (0.53 ± 0.02 to 1.02 ± 0.17 mm). The 3DFC shifts the passive pressure volume loop toward the pressure axis but does not alter left ventricular (LV) ejection fraction, systolic displacement, LV end-diastolic pressure/dimension, or LV cavity area. The 3DFC stimulates selected cytokine activation with a decrease in the proinflammatory cascade and increased total protein content stimulated by strained 3DFC *in vitro*.
Conclusion: The 3DFC functions as a cell delivery device providing matrix support for resident cell survival and integration into the heart. The imbedded fibroblasts of the 3DFC release a complex blend of cardioactive cytokines promoting increases in microvessel density and anterior wall blood flow but does not improve ejection fraction or alter LV remodeling.

Introduction

Cell-based regenerative therapies have been explored recently as a treatment for myocardial infarction (MI) with mixed results.[1–3] Basic laboratory work shows dramatic increases in left ventricular (LV) function and survival. Meanwhile, clinical trials demonstrate that intracoronary delivery of cells is safe, well tolerated, and results in modest improvements in LV function.[4–10] However, few studies focus on chronic heart failure (CHF), which affects nearly 5 million Americans with an estimated 500,000 new diagnoses annually. Fewer than 50% of patients found to have CHF survive more than 5 years.[11] Current clinical treatments focus on stabilizing CHF and preventing further deterioration; they neither stimulate angiogenesis nor regenerate myocytes or restore the lost functional and structural elements of the heart.[12–14] Studies evaluating cell-based therapies in CHF are generally nonconclusive showing 2%–3% increases in ejection fraction (EF)[10] including studies of skeletal myoblast injections in patients with ischemia undergoing coronary artery bypass grafting (CABG) that show no improvement in LV function.[15]

While enthusiasm for cell-based therapy for heart failure remains high, the limited clinical beneficial effects may be because most transplanted cells do not survive when injected into the infarcted heart.[16–18,45] Alternatively, new cell-based delivery techniques using bioengineered patches are evolving.[19–21] Previously, our laboratory[22] evaluated a biodegradable three-dimensional fibroblast construct (3DFC) composed of a matrix-embedded human newborn dermal fibroblasts cultured onto a vicryl mesh to produce a living, metabolically active tissue. The 3DFC secretes angiogenic growth factors, including hepatocyte growth factor (HGF), vascular endothelial growth factor (VEGF), and basic

[1]Department of Cardiology, Southern Arizona VA HealthCare System, Tucson, Arizona.
[2]Department of Life Sciences, Arizona State Univeristy, Tempe, Arizona.
[3]College of Medicine, University of Arizona, Phoenix, Arizona.
[4]Banner SunHealth Research Institute, Sun City, Arizona.
[5]Development Engineering Sciences, Flagstaff, Arizona.

fibroblast growth factor (bFGF) (Table 4), which have been shown to increase new blood vessel formation *in vivo*.[23–25]

In this study, the 3DFC was evaluated in a rat CHF model. Echocardiography was employed for evaluation of EF, systolic displacement, and LV end systolic and diastolic diameter. We used solid-state micromanometers to obtain hemodynamic data. Structural improvements were verified using histological methods. Extensive investigation evaluated both the *in vivo* and *in vitro* angiogenic properties of the 3DFC. Lastly, the 3DFC's proinflammatory markers were evaluated in strained versus static culture conditions *in vitro*.

Materials and Methods

Experimental design and treatment groups

Normal adult male Sprague-Dawley rats underwent left coronary artery ligation and were randomized to sham or 3DFC placement 3 weeks after surgery with three treatment groups: Sham, CHF, and CHF + 3DFC. The experiments were performed in an Association for Assessment and Accreditation of Laboratory Animal Care International (AAALAC)-accredited facility with approval from animal use committees of Southern Arizona Veterans Administration Health Care System (SAVAHCS) and the University of Arizona.

Coronary artery ligation experimental MI

The rat coronary artery ligation model is standard in our laboratory.[22,26–32] Rats were anesthetized with ketamine and acepromazine, a left thoracotomy was performed, the heart expressed from the thorax, and a ligature was placed around the proximal left coronary artery. The rats were maintained on standard rat chow, water *ad libitum*, and pain medication postoperatively.

The 3DFC patch

The 3DFC is a cryopreserved human fibroblast, extracellular matrix, on a bioabsorbable scaffold[22,33,34] (Supplemental Fig. S1, available online at www.liebertonline.com/ten). The fibroblast cells are tested for animal viruses, retroviruses, cell morphology, karology, isoenzymes, and tumorgenicity and free from viruses, retroviruses, endotoxins, and mycoplasma. The 3DFC was provided by Theregen, Inc., and is frozen ($-75^{\circ}C \pm 10^{\circ}C$) in pieces 5×7.5 cm with an average thickness of 200 micrometers. The 3DFC was thawed in phosphate buffered saline (34°C–37°C), handled gently by the edges to limit cellular damage, and applied to the heart within 60 min of being removed from its container (Supplemental Fig. S2A, available online at www.liebertonline.com/ten). The 3DFC does not generate an immune response in previous work[22,33–35] (Investigators' brochure ITT-101; Theregen), or in current clinical studies (data not published). The low immunogenicity of allogeneic fibroblasts may be because these fibroblasts show little induction of cluster of differentiation (CD)40 and human leukocyte antigen-DR (HLA-DR) in response to γ-interferon.[35]

Hemodynamic measurements in vivo

Using standard techniques developed in our laboratory, rats were anesthetized with inactin (100 mg/kg intraperitoneal injection), placed on a specially equipped operating table with a heating pad, intubated, and placed on a rodent ventilator with a 2F solid state micromanometer tipped catheter with two pressure sensors (Millar Instruments, Inc.) inserted via the right femoral artery, with one sensor located in the left ventricle and another in the ascending aorta. The pressure sensor is equilibrated in 37°C saline, and LV and aortic pressures/heart rate were recorded, digitized at a rate of 1000 Hz to calculate LV dP/dt and the time constant of LV relaxation or tau.[22,26,29–32,36]

LV pressure–volume relationships in vitro

We measured LV pressure–volume (PV) relations with the heart arrested with potassium chloride, and a PE-90 catheter with telescoped PE-10 tubing inside, inserted into the LV via the aortic root. One end of the double-lumen LV catheter was connected to a volume infusion pump (Harvard Apparatus), whereas the other end was connected to a pressure transducer zeroed at the level of the heart. The right ventricle was partially incised to prevent loading on the left ventricle. The LV was filled (1.0 mL/min) to 60–100 mmHg and unfilled while pressure was recorded onto a physiologic recorder (Gould Electronics); ischemic time from euthanasia to the PV curves was limited to 10 min; the volume infused is a function of filling rate.[22,27,28]

From the pressure–volume data recorded *in vivo*, the stiffness constants K_0, K_1, K_2, K_3, and K_4 are determined by methods described previously by our laboratory.[30] In brief, pairs of simultaneous pressure–volume points (15 pairs for each pressure interval) were obtained. The stiffness constants were calculated with the following analysis: the pressure–volume data are fitted to the exponential equation $P = P_0 e^{KV}$ (pressure is assumed to be equal to P_0 when volume is zero). Thus, $\ln P = \ln P_0 + KV$, and when lnP was plotted versus V, K is the slope of this relation. The overall stiffness constant was K_0 (2.5–30 mmHg). K_1 (0–3 mmHg), K_2 (3–10 mmHg), K_3 (10–20 mmHg), and K_4 (20–30 mmHg) were derived.

Echocardiography

We performed closed chest transthoracic echocardiography using a Vingmed, Vivid 7 system echo machine (GE Ultrasound) with EchoPac (GE Ultrasound) programming software with a 10 MHz multiplane transducer with views in the parasternal short axis and long axis, to evaluate the anterior, lateral, antero-lateral, inferior, and posterior walls. Systolic displacement of the anterior wall and EF were obtained from 2D and M-mode measurements of myocardial wall thickness and LV dimensions. Systolic displacement is a measure of focal LV wall thickening; from the M mode through the anterior wall, the difference in the thickness between systole and diastole is the systolic displacement. This was used to quantify focal LV wall systolic function with particular reference to this study where we measure systolic displacement of the anterior infarcted wall.[22,32]

Myocardial perfusion

We used neutron-activated microspheres (BioPal, Inc.) to measure myocardial blood flow. The isotopes were injected, and a tissue sample was obtained, and at a later time activated with the emitted radiation measured with high resolution detection equipment.[22,37–39] Three separate isotopes

(lutetium, gold, and samarium) were injected: one at baseline before coronary ligation, one immediately after ligation at the time of the acute MI, and one at 6 weeks in separate groups of rats with CHF, and with CHF + 3DFC. For each measurement 750,000 nonradioactive elementally labeled 15 μm microspheres (V = 300 μL) from Biopal, Inc., were injected into the left ventricle transapically with a 1 cc syringe and 27-gauge needle. At the terminal study point, tissues were harvested, oven-dried, and collected for analysis. At the time of microsphere injection we performed a transthoracic echocardiogram to measure stroke volume and calculate cardiac output as stroke volume×heart rate. Assuming that 4% of the cardiac output perfuses the coronary arteries,[39] we know the total myocardial blood flow. The microspheres deposited in the anterior wall represent the percentage of blood flow down the left coronary artery to the anterior wall at each time point.[22]

Microvessel histopathology

Hearts were formalin fixed (10%) before paraffin embedding. Heat-induced epitope retrieval of 3-μm-thick sections was performed in citrate-based Diva buffer (pH 6.2) for 1 min at 125°C using a Decloaker pressure cooker (Biocare Medical). We used single immunohistochemical staining for anti-rabbit factor VIII (Dako) (1:1000) to perform histological analysis of microvessel density defined by light microscopy at 40×magnification. The number of cross-sectional vessels per field was counted by two people blinded to treatment, and average measurements from six different fields were recorded for each value. Knowing the area of the optical field, data were reported as number of vessels/μm^2.

Fibroblast identification histopathology

Rodent heart samples were processed and embedded into paraffin for subsequent 5 μm sectioning. Vimentin antibody was purchased from Santa Cruz Biotechnology (cat# sc-32322) and used at a 1:100 dilution in blocking solution. Heat antigen retrieval using citrate buffer was applied before blocking incubation. Primary antibody was incubated overnight. An ABC system from Vector Laboratories was used to amplify the signal with subsequent peroxidase 3,3′-diaminobenzidine (DAB) treatment. Light methyl green was used as a background counterstain.

Trichrome staining

Cut sections were deparaffinized and incubated in potassium dichromate-hydrochloric acid solution, stained with acid fuchsin, fixed with phosphomolybdic acid solution, and stained with orange G. Lastly, sections were treated with aqueous acetic acid, aniline blue, and acetic acid; rinsed with EtOH; and dehydrated in absolute alcohol.

Left ventricle measurements

We injected 40 meq/mL potassium chloride into the right ventricle to arrest the heart in diastole. A bolus of 1 mL per 100 g of body weight was rapidly injected into the right ventricle, effecting arrest. Images of trichrome-stained heart sections were captured around the entire circumference of a mid-LV cross-sectional slice. Calibrated, scaled, individual images were stitched together using imaging processing software (Adobe Photoshop Elements). Measurements of each heart were taken using image analysis software (NIH Image J 1.39u), again calibrated from images with a standardized micrometer. The average of three measurements for each heart was taken to represent the wall thickness and LV cavity area value for each heart. Five animals were evaluated from each treatment group (CHF vs. CHF+3DFC).

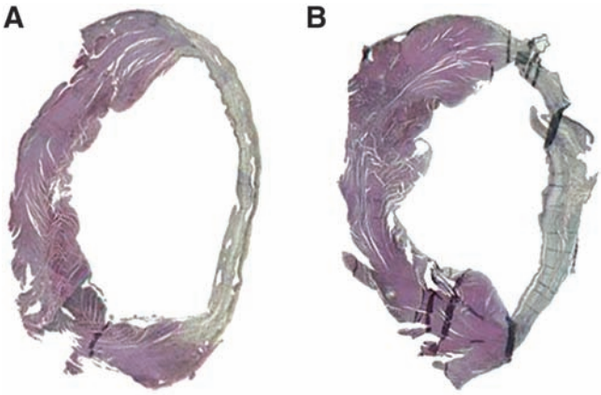

FIG. 1. Trichrome-stained left ventricular (LV) sections of (**A**) chronic heart failure (CHF) versus (**B**) three-dimensional fibroblast-construct (3DFC)-treated CHF hearts. The 3DFC increases LV wall thickness in treated versus untreated hearts.

Biomechanical strain induced cytokine secretion

The 3DFC were attached to BioFlex® collagen-coated membranes using a waterproof adhesive and incubated in a medium containing 2% fetal bovine serum for 24 h. The

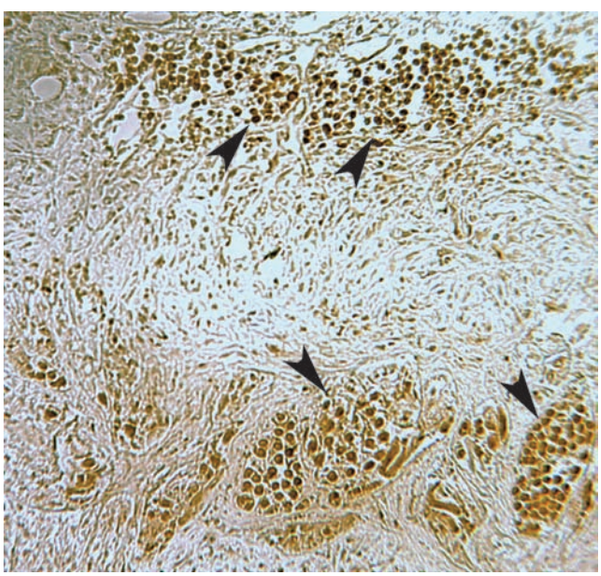

FIG. 2. Positive human-specific vimentin antibody staining demonstrates presence of the 3DFC's resident fibroblasts 3 weeks after implantation into a rat CHF model. Arrows illustrate positive human fibroblasts staining. Scale bar = 100 μm.

Table 1. Hemodynamics Three-Dimensional Fibroblast Construct in Rats with Chronic Heart Failure

	MAP (mmHg)	*Tau (ms)*	*HR (bpm)*	*LV SP (mmHg)*	*LVEDP (mmHg)*	*+LV dP/dt (mmHg/s)*	*−LV dP/dt (mmHg/s)*	*PDP (mmHg)*
Sham	135 ± 7	19.8 ± 3.6	297 ± 24	152 ± 12	5.6 ± 1.8	8091 ± 1050	6396 ± 1237	198 ± 19
CHF	105 ± 6^a	31.2 ± 4.5^a	270 ± 33	116 ± 7^a	23.4 ± 2.2^a	5153 ± 590^a	3111 ± 651^a	121 ± 7^a
CHF+3DFC	95 ± 19^a	30.6 ± 7.6^a	270 ± 28	113 ± 24^a	22.3 ± 6.6^a	4961 ± 1127^a	3035 ± 763^a	132 ± 26^a

Values are mean ± SD; sham, $n = 5$; CHF, $n = 5$; CHF+3DFC, $n = 10$.
[a]$p < 0.05$ versus sham.
CHF, chronic heart failure; 3DFC, three-dimensional fibroblast construct; LV, left ventricle; MAP, mean arterial pressure; HR, heart rate; LVSP, left ventricular systolic pressure; LVEDP, left ventricular end diastolic pressure; +/− LV dP/dt, left ventricular derivative pressure/derivative time; PDP, peak developed pressure.

3DFC were equilaxially strained using a flexercell apparatus at 10% 1 Hz for 48 h to model an *in vivo* cardiac cycle. Conditioned medium samples were collected, and secreted peptides were identified and quantified via protein microarrays (RayBiotech Inc.). Fibroblast proliferation was assayed via dsDNA and total cellular protein concentration was assayed calorimetrically. Peptides were normalized in pg/mL per dsDNA concentration.

Statistical analysis

Data were expressed as mean ± standard error. For the physiologic and echocardiographic measurements, the Student *t*-test was used for single comparison of sham versus other study groups. Interactions were tested using two-way analysis of variance; intergroup differences were evaluated using the Student-Newman-Keuls test for statistical significance ($p \leq 0.05$). Pressure–volume relations were evaluated using multiple linear and polynominal regression analysis. The correlation of statistical difference was based on the Durbin-Watson statistic, F-statistic, *p*-value, and variance coefficients.

Results

In our laboratory the rat coronary artery ligation model results in about a 40%–50% operative mortality to produce large infarcts with LV end-diastolic pressures >20 mmHg.[30,31] Supplemental Figure S2 shows the 3DFC before implantation (A), with the chest reopened in a rat with an infarcted dilated heart 3 weeks after left coronary artery ligation (B), and the 3DFC implanted on this infarcted heart 3 weeks after MI (C).

LV dimensions

Echocardiography and immunohistochemistry were employed to detect functional and structural improvements in CHF groups treated with 3DFC. In a rat model of CHF, classically, there is a decrease ($p < 0.05$) in LV EF (75% ± 2% to 35% ± 3%) with CHF; placement of the 3DFC does not restore EF (35% ± 5%) at 6 weeks (Supplemental Fig. S3A, available online at www.liebertonline.com/ten). In addition, regional LV function, defined as systolic displacement of the infarcted anterior wall, does not increase with the 3DFC (Supplemental Fig. S3B, available online at www.liebert online.com/ten).

The LV end-systolic and end-diastolic diameters increase almost twofold ($p < 0.05$) in CHF from 0.39 ± 0.03 to 0.66 ± 0.10 cm and from 0.64 ± 0.04 to 0.93 ± 0.05 cm in CHF, respectively (Supplemental Fig. S4A, B, available online at www.liebertonline.com/ten). Placement of the 3DFC in CHF rats does not change the end-systolic (0.77 ± 0.04 cm) or end-diastolic dimension (0.90 ± 0.04 cm). Histological assessment reveals an increase in anterior wall thickness (Supplemental Fig. S5, available online at www.liebertonline.com/ten, and Fig. 1) with implantation of the 3DFC from $0.53 + 0.02$ to $1.02 + 0.17$ mm (Fig. 1 A, B) but does not decrease LV cavity area ($37.89 + 3.72$ to $38.46 + 5.17$ mm^2). Human-specific vimentin staining demonstrated resident fibroblasts from the 3DFC were present within the epicardial section of LV 3 weeks after implantation (Fig. 2).

LV hemodynamics

Solid-state micromanometer catheters were placed in the LV and ascending aorta to evaluate LV hemodynamic changes. These data show what we and other laboratories have shown: rats with CHF, 6 weeks after left coronary artery ligation with a threefold increase in LV end diastolic pressure, a 23% reduction in LV systolic blood pressure, a 22% reduction in mean arterial blood pressure, a 36% reduction in positive LV dP/dt, a 50% reduction in negative LV dP/dt, a 40% decrease in peak developed pressure, and a 60% increase in tau ($p < 0.05$), the time constant of LV relaxation (Table 1). Implanting the 3DFC does not significantly ($p < 0.05$) change any hemodynamic parameters described above. There is an increase ($p < 0.05$) in right

Table 2. Heart Weights Three-Dimensional Fibroblast Construct in Rats with Chronic Heart Failure

	Body weight (g)	*Right ventricle (g)*	*Left ventricle (g)*	*Heart weight/body weight ratio*
Sham	351 ± 222	0.21 ± 0.03	0.82 ± 0.17	0.23 ± 0.04
CHF	353 ± 35	0.38 ± 0.13^a	0.83 ± 0.12	0.24 ± 0.03
CHF+3DFC	342 ± 26	0.28 ± 0.08	0.81 ± 0.11	0.24 ± 0.04

Values are mean ± SD; sham, $n = 5$; CHF, $n = 5$; CHF+3DFC, $n = 10$.
[a]$p < 0.05$ versus sham.

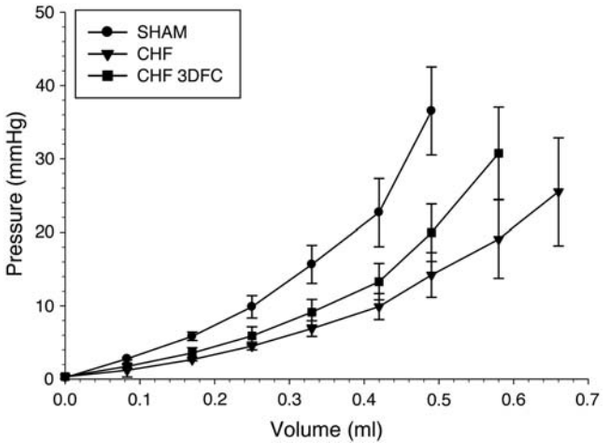

FIG. 3. Pressure–volume curves in sham, CHF, and CHF 3DFC. The 3DFC shifts the CHF pressure–volume curve ($p < 0.05$) to the left toward the pressure axis. Sham, $n = 5$; CHF, $n = 5$; CHF+3DFC, $n = 8$.

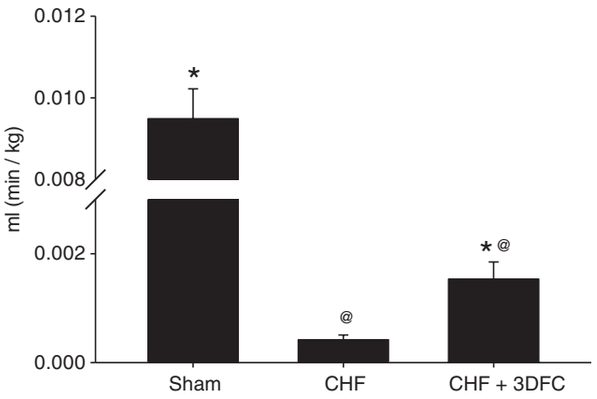

FIG. 4. Anterior wall myocardial blood flow in treated (3DFC) versus control groups. Data are mean + standard error. $^{*}p < 0.05$ as compared to 6-week CHF. $^{@}p < 0.05$ compared to sham. The 3DFC improves blood flow in the infarcted wall in rats with CHF. Sham, $n = 12$; 6-week CHF, $n = 8$; 6-week CHF+3DFC, $n = 13$.

ventricular weight in the CHF rats (Table 2). Thus, implanting the nonviable 3DFC has no effect on any hemodynamic parameter.

Pressure–volume loops

The PV relationship shows dilatation of the left ventricle in CHF; the 3DFC patch attenuates this dilatation with a shift to the left ($p < 0.05$) toward the pressure axis (Fig. 3). The overall LV chamber stiffness constant (K_0) decreases ($p < 0.05$, Table 3) with CHF and returns toward sham with 3DFC (Table 3).

Myocardial blood flow and vessel density

To determine if the 3DFC revascularized ischemic tissue, myocardial blood flow was evaluated using neutron-activated microspheres. Myocardial blood flow to the anterior infarcted wall decreases ($p < 0.05$) in CHF; the 3DFC increases ($p < 0.05$) myocardial blood flow in 3DFC-treated groups (Fig. 4). Additionally, using immunohistochemistry, we evaluated microvessel density formation within the epicardial infarct and peri-infarct zones. Factor VIII staining (Fig. 5) reveled an increase ($p < 0.05$) in microvessel density in groups treated with 3DFC (Fig. 6).

Table 3. Left Ventricular Chamber Stiffness Constants in Sham, Chronic Heart Failure, and Chronic Heart Failure+Three-Dimensional Fibroblast Construct Rats

	Sham	*CHF*	*CHF+3DFC*
K_0 (2.5–30 mmHg)	5.86 ± 0.37	4.78 ± 0.31^{a}	5.24 ± 0.48
K_1 (0–3 mmHg)	7.57 ± 0.78	5.95 ± 0.86	7.10 ± 0.86
K_2 (3–10 mmHg)	5.08 ± 0.62	4.53 ± 0.27	5.16 ± 0.86
K_3 (10–20 mmHg)	5.70 ± 0.64	5.03 ± 0.31	5.07 ± 0.64
K_4 (20–30 mmHg)	5.82 ± 1.02		4.78 ± 0.76

Values are mean ± standard error; sham, $n = 5$; CHF, $n = 5$; CHF/3DFC, $n = 10$. K_4 was not calculated for CHF because $n = 2$.
$^{a}p < 0.05$ versus sham.

Strain induced cytokine stimulation

In an effort to understand the cytokine production of the 3DFC, selected angiogenic cytokines were measured (*in vitro*) in control (static) versus strained settings. Measurable amounts of monocyte chemoattractant protein-1 (MCP-1), HGF, interleukin-8 (IL-8), interferon-γ, tumor necrosis factor-α, Angiogenin, VEGF, IL-1α, bFGF, Leptin, IL-1β, IL-4, IL-6, platelet-derived growth factor-BB, placental growth factor, and epidermal growth factor (EGF) were detected in conditioned medium samples from both control and strained 3DFC. Strain significantly ($p < 0.05$) decreased extracellular concentrations of interferon-γ, tumor necrosis factor-α, IL-1α, IL-1β, IL-4, and EGF. No appreciable angiopoietin-2 (Ang-2), heparin-binding EGF-like growth factor, IL-10, or IL-13 was detected in any samples (Table 4). In addition, equilbiaxial strain showed no significant ($p < 0.05$) change in dsDNA concentration; however, total protein content was significantly ($p < 0.05$) elevated with strain 2.32 ± 0.3 versus $3.44 \pm 0.3\,\mu g/mL$.

Discussion

Our work demonstrates that implanting a viable fibroblast matrix patch in rats with CHF increases LV wall thickness and induces angiogenesis with a resultant increase in myocardial blood flow in the area of previous infarction. In addition, the 3DFC improves passive filling of the LV but does not contribute to improvement in EF or attenuate LV remodeling. Although the mechanisms responsible for the increase in myocardial blood flow and capillary density are not clear, we do show that 3DFC induces selective paracrine activation *in vitro* that may explain part of its benefit.

Previous work by our laboratory shows that when 3DFC is implanted acutely after MI, the patch improves myocardial blood flow, LV function, and also partially reverses LV remodeling.[22] It is unclear why the 3DFC, when implanted in rats with CHF, does not restore LV function or reverse LV remodeling. Acute placement of the 3DFC results in significant revascularization and restored blood flow to potentially

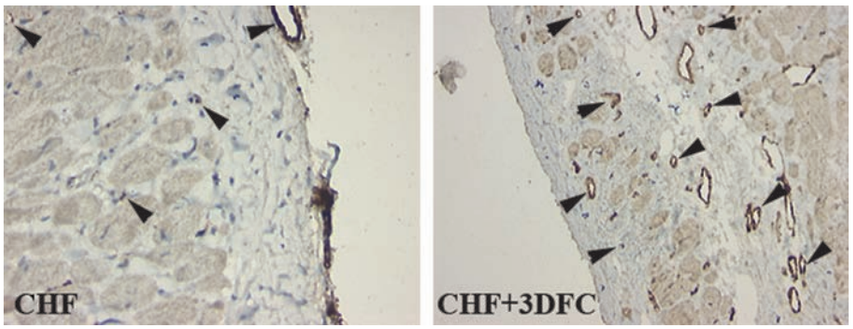

FIG. 5. Factor VIII staining showing more staining, that is, increased vessel density with the 3DFC in CHF rats. Arrowheads indicate positively stained (brown) microvessel (40×).

stunned myocardium, possibly preserving tissue viability. However, if the 3DFC is placed in CHF after infarct expansion and scar development has already occurred, although the 3DFC still induces angiogenesis, the adverse LV remodeling cannot be reversed, at least not in the 3-week time frame, that is effective in an acute MI.[22]

Ex vivo *pressure relationship versus* in vivo *analysis*

The 3DFC treatment shifts the PV relationship to the left, toward the pressure axis; however, the 3DFC had no change on LV end systolic or diastolic diameter. To explain this contradiction, echocardiography data were collected *in vivo*, while PV loop data were collected *ex vivo*. To measure the PV relation *ex vivo*, hearts were arrested in diastole using KCL, while left ventricular end diastolic diameter (LVEDD) was measured *in vivo* while the heart may not have been completely relaxed due to incomplete diastole and/or the presence of pericardium, which is typically removed during *ex vivo* preparation.

Paracrine activation

The 3DFC is a viable construct composed of a matrix, embedded with human newborn dermal fibroblasts cultured *in vitro* onto a bio-absorbable mesh to produce a living, metabolically active tissue that secretes growth factors (Table 4) but engendering no immune response.[35] The fibroblasts proliferate across the mesh (Supplemental Fig. S1) and secrete human dermal collagen, fibronectin, and glycosaminoglycans, embedded in a self-produced dermal matrix. Although the mechanisms of action of cell-based therapy are not clear, most investigators believe that paracrine stimulation from the cells themselves may be responsible for the beneficial effects. Paracrine stimulation has been shown to result in cardioprotection of the cardiomyocytes at the cellular level.[40] The 3DFC releases a complex blend of cardioactive cytokines (Table 4) with well-documented roles in regulating ventricular function, blood flow, and vessel density. The functional dynamics of some cytokines are potentially stimulated by other active peptides as well as interpolated environmental conditions, as in the case with the peptide MCP-1 acting together with IL-8 to enhance the metastatic migration of mural cells toward endothelial cells, promoting both the maturation of new blood vessels and arteriogenesis.[41–43] In hyperemic flow conditions, but not at rest, MCP-1 and Leptin increase collateral blood flow.[43] We measured several potent angiogenic growth factors secreted from the 3DFC in high concentrations, including HGF, VEGF, angiogenin, and bFGF. The HGF induces powerful mitogenic activity on endothelial cells, and increases blood vessel number when introduced into infarcted canine myocardium.[23] VEGF and bFGF bind to cell-surface-expressed receptors equipped with tyrosine kinase activity leading to improvements in LV remolding and myocyte hypertrophy.[24] VEGF also increases functional improvement of post-infarcted hearts.[25] Interestingly, our data show that the imbedded fibroblasts of the 3DFC response to biomechanical strain results in an increase in total protein, which may be due to upregulation of intracellular proteins such as actin, or an increase in extracellular matrix proteins such as collagen, elastin, and fibronectin, providing structural support and a scaffolding for cellular migration aiding in cardiac growth. In addition, these data show that strain decreased the fibroblasts' secretion of proinflammatory molecules (Table 4), and suggest the possibility that heart rate and force of contraction may modify the peptide secretory profile of 3DFC. Mechanotransduction of human fibroblasts in 3D constructs have been investigated by others and supports these findings.[44] This described paracrine effect does not occur with the nonviable 3DFC (data not shown) presumably because the nonviable 3DFC does not contain living fibroblasts. Previous work in rats and mice has shown that implanting

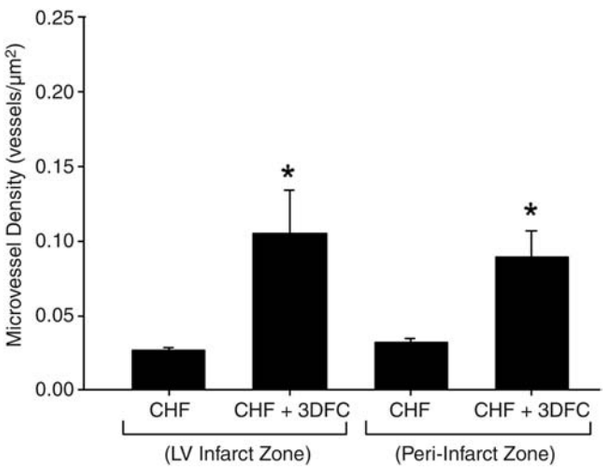

FIG. 6. Data are mean ± standard error. CHF (LV Infarct Zone), $n = 5$; CHF+3DFC (LV Infarct Zone), $n = 9$; CHF (Peri-Infarct Zone), $n = 5$; CHF+3DFC (Peri-Infarct Zone), $n = 9$. *$p < 0.05$ as compared to baseline CHF.

Table 4. Cytokine Activation in Static (Control) Versus Strained Three-Dimensional Fibroblast Construct Patches

	Static/control	*Strain*
Angiogenesis		
Angiogenin	1322 ± 769.1	383.4 ± 140.0
Angiopoientin-2	−71.39 ± 182.7	−180.8 ± 99.96
Basic fibroblast growth factor	460.9 ± 289.6	38.24 ± 50.28
Endothelial growth factor	15.39 ± 0.6515	5.381 ± 3.382
Heparin-binding endothelial growth factor	−226.1 ± 189.0	−171.9 ± 49.39
Hepatocyte growth factor	9725 ± 4307	9285 ± 5219
Leptin	−152.1 ± 3610	458.7 ± 1970
Platelet-derived growth factor BB	37.56 ± 7.660	23.46 ± 4.286
Placental growth factor	11.12 ± 4.252	27.36 ± 13.77
Vascular endothelial growth factor	324.3 ± 151.5	758.3 ± 392.0
Inflammation		
Interferon-γ	3573 ± 257.5	2060 ± 152.8[a]
Interleukin-1α	576.5 ± 23.13	211.5 ± 6.092[a]
Interleukin-1beta	170.8 ± 27.12	36.38 ± 5.152[a]
Interleukin-4	101.0 ± 15.55	36.22 ± 7.121[a]
Interleukin-6	82.69 ± 33.13	36.05 ± 19.28
Interleukin-8	3937 ± 2192	2966 ± 1517
Interleukin-10	−20.16 ± 14.37	−47.89 ± 8.051
Interleukin-13	−77.46 ± 35.06	−136.9 ± 34.37
Monocyte chemotactic protein-1	11900 ± 5890	10830 ± 2847
Tumor necrosis factor-α	2183 ± 99.86	1277 ± 110.8[a]

Cytokine, chemokine, and growth factor stimulation of angiogenic and inflammatory markers in static (control) versus strained 3DFC patches *in vivo* over 48 h (10% 1 Hz). Expression in pg cytokine/μg DNA, $n = 3$. Adjusted for 2% fetal bovine serum media.

[a]$p < 0.05$ versus control.

the nonviable 3DFC does not improve myocardial blood flow or improve LV function.[22,33,34] Thus, the benefits from the 3DFC are due to more than just the physical presence and the restraining effects of the patch.

Using the 3DFC as a delivery system

Although this present report outlines the use of the 3DFC by itself, as treatment for CHF, the fibroblast patch could be used as an adjuvant delivery system for cell-based therapy. Because patients in heart failure present in the chronic phase of their disease, this could be an elective procedure where cells are harvested, grown in culture, seeded on the 3DFC, and reimplanted in the patient.

With direct cell injection into the heart, the majority of transplanted cells do not survive.[16–18] The lack of survival of these injected cells is related, in part, to an inadequate blood supply and inadequate matrix support for the new cells. The injected cells are fragile, resulting in cell aggregation due to lack of physical support for the cells to attach to the tissue extracellular matrix. This 3D scaffold offers a potential solution to the problem of an inadequate cellular support structure (Supplemental Fig. S1). In addition, Figure 7 demonstrates the integration of the 3DFC into the infarcted tissue and remnants of the vicryl mesh support structure 3 weeks after implantation.

Conclusion

We report induced angiogenesis, LV wall thickening, and improvements in myocardial blood flow as well as passive LV filling, without reversal of EF or LV remodeling using the viable 3DFC implanted in rats with ischemia-induced CHF. Our concept is that the 3DFC provides a support structure that allows cells to grow into the damaged heart and create new blood vessel growth, resulting in increased myocardial blood flow. In addition, treatment with the 3DFC increases ventricular wall thickness. With the limited success of current approaches of direct cell injection into the heart, the

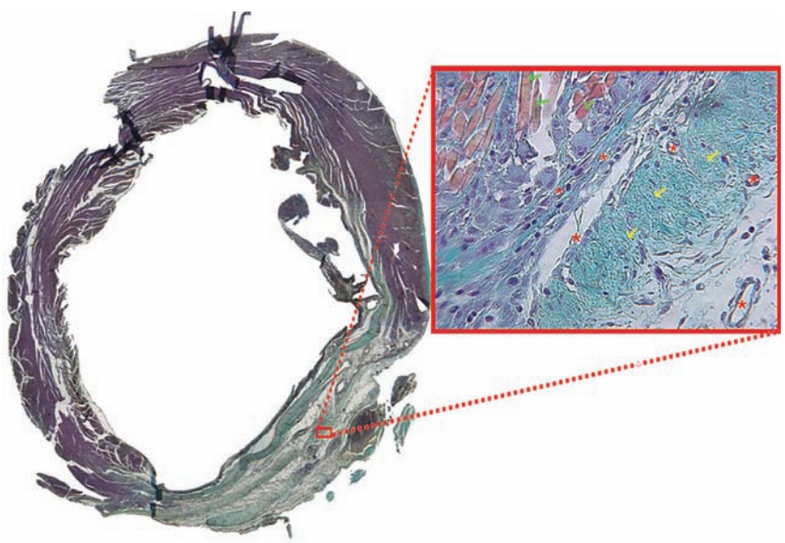

FIG. 7. Trichrome-stained LV cross section of a 3DFC-treated CHF heart. Higher magnification image inset highlighted in red; green arrows indicate remnants of vicryl mesh, yellow arrows indicate collagen fibers, and red asterisks indicate microvasculature. Within 3 weeks, the 3DFC vicryl mesh fibers have incorporation into the anterior wall.

3DFC represents a potentially new approach to cell-based therapy for CHF. The advantage of using the 3DFC is that it is an off-the-shelf product, does not generate an immune response, and can be delivered with a minimally invasive approach in patients. While we have used the 3DFC alone, this matrix patch could be viewed as a delivery system for cell-based therapy for heart failure where specific cells could be seeded on the 3DFC before implantation on the heart.

Acknowledgments

We acknowledge Nicholle Johnson, B.S., Howard Byrne, and Maribeth Stansifer, B.S., for their technical work, and Dr. Tom Raya, M.D., for his advice and counsel. This study was supported by the Department of Veterans Affairs, the WARMER Foundation, The Hansjörg Wyss Foundation, the Arizona Biomedical Research Commission, and the Biomedical Research and Education Foundation of Southern Arizona.

Disclosure Statement

Theregen, Inc., provides the 3DFC patch but does not provide any financial support for these studies. The University of Arizona has a Memorandum of Understanding with the Department of Veteran Affairs and has a licensing agreement with Theregen to use the 3DFC patch in the heart. For this study, Theregen provided only the 3DFC patch. Theregen did not provide any financial support. Dr. Thai is a consultant for Theregen, Inc. Drs. Goldman and Kellar are nonpaid members of the Scientific Advisory Board for Theregen. No competing financial interests exist with any of the other authors.

References

1. Orlic, D., Kajstura, J., Chimenti, S., Jakoniuk, I., Anderson, S.M., Li, B., Pickel, J., McKay, R., Nadal-Ginard, B., Bodine, D.M., Leri, A., and Anversa, P. Bone marrow cells regenerate infarcted myocardium. Nature **410,** 701, 2001.
2. Balsam, L.B., Wagers, A.J., Christensen, J.L., Kofidis, T., Weissman, I.L., and Robbins, R.C. Haematopoietic stem cells adopt mature haematopoietic fates in ischaemic myocardium. Nature **428,** 668, 2004.
3. Murry, C.E., Soonpaa, M.H., Reinecke, H., Nakajima, H., Nakajima, H.O., Rubart, M., Kishore, B., Pasumarthi, S., Virag, J.I., Barteimez, S.H., Poppa, V., Bradford, G., Dowell, J.D., Williams, D.A., and Filed, L.J. Haematopoietic stem cells do not transdifferentiate into cardiac myocytes in myocardial infarcts Nature **428,** 664, 2004.
4. Schächinger, V., Assmus, B., Britten, M.B., Honold, J., Lehmann, R., Teupe, C., Abolmaali, N.D., Vogl, T.J., Hofmann, W.K., Martin, H., Dimmeler, S., and Zeiher, A.M. Transplantation of progenitor cells and regeneration enhancement in acute myocardial infarction. Final one-year results of the TOPCARE-AMI trial. J Am Coll Cardiol **44,** 1690, 2004.
5. Wollert, K.C., Meyer, G.P., Lotz, J., Rings-Lichtenberg, S., Lippolt, P., Breidenbach, C., Fichtner, S., Korte, T., Horing, B., Messinger, D., Arseniev, L., Ganser, A., and Drexler, H. Intracoronary autologous bone-marrow cell transfer after myocardial infarction: the BOOST randomized controlled clinical trial. Lancet **364,** 141, 2004.
6. Strauer, B.E., Brehm, M., Zeus, T., Bartsch, T., Schannwell, C., Antke, C., Sorg, R.V., Kogler, G., Werner, P., Muller, H.W., and Kostering, M. Regeneration of human infarcted heart muscle by intracoronary autologous bone marrow cell transplantation in chronic coronary artery disease. The IACT study. J Am Coll Cardiol **46,** 1651, 2005.
7. Assmus, B., Honold, J., Schachinger, V., Britten, M.B., Fischer-Rasaokat, U., Lehmann, R., Teupe, C., Pistorius, K., Martin, H., Abolmaali, N.D., Tonn, T., Dimmeler, S., and Zeiher, A. Transcoronary transplantation of progenitor cells after myocardial infarction. N Engl J Med **355,** 1222, 2006.
8. Janssens, S., Dubois, C., Bogaert, J., Theunissen, K., Deroose, C., Desmet, W., Kalantzi, M., Herbots, L., Sinnaeve, P., Dens, J., Maertens, J., Rademakers, F., Dymarkowski, S., Gheysens, O., Van Cleemput, J., Bormans, G., Nuyts, J., Belmans, A., Mortelmans, L., Boogaerts, M., and Van de Werf, F. Autologous bone marrow-derived stem-cell transfer in patients with ST-segment elevation myocardial infarction; double blind, randomized controlled trial. Lancet **367,** 113, 2006.
9. Lunde, K., Solheim, S., Aakhus, S., Arnesen, H., Abdelnoor, M., Egeland, T., Endresen, K., Ilebekk, A., Mangschau, A., Fjeld, J.G., Smith, H.J., Taraldsrud, E., Grøgaard, H.K., Bjørnerheim, R., Brekke, M., Müller, C., Hopp, E., Ragnarsson, A., Brinchmann, J.E., and Forfang, K. Intracoronary injection of mononuclear bone marrow cells in acute myocardial infarction. N Engl J Med **355,** 1199, 2006.
10. Schächinger, V., Erbs, S., Elsässer, A., Haberbosch, W., Hambrecht, R., Hölschermann, H., Yu, J., Corti, R., Mathey, D.G., Hamm, C.W., Süselbeck, T., Werner, N., Haase, J., Neuzner, J., Germing, A., Mark, B., Assmus, B., Tonn, T., Dimmeler, S., and Zeiher, A.M. Intracoronary bone marrow-derived progenitor cells in acute myocardial infarction: a randomized, double-blind, placebo controlled multicenter trial (REPAIR-AMI). N Engl J Med **355,** 1210, 2006.
11. Heart Failure Society of America. Quick Facts & Questions about Heart Failure. Available at http://hfsa.org/heart_failure_facts.asp, 2010.
12. Hendrikx, M., hensen, K., Clijsters, C., Jongen, H., Koninckx, R., Bijnens, E., *et al.* Recovery of regional but not global contracile function by the direct intramyocardial autologous bone marrow transplantation: results from a randomized controlledclinical trial. Circulation **114(Suppl 1),** 1101, 2006.
13. Ang, K.L., Chin, D., Leyva, F., Foley, P., Kubal, C., Chalil, S., *et al.* Randomized, controlled trail of intramuscular or intracoronay injection of autolgous bone marrow cell into scarred myocardium during CABG versus CABG alone. Nat Clin Pract Cardiovasc Med **5,** 663, 2008.
14. Bel, A., Messas, E., Agbulut, O., Richard, P., Samuel, J.L., Bruneval, P., *et al.* Transplantation of autologous fresh bone marrow into infarcted myocardium: a word of caution. Circulation **108(Suppl 1),** 11247, 2003.
15. Menasché, P., Alfieri, O., Janssens, S., McKenna, W., Reichenspurner, H., Trinquart, L., Vilquin, J.T., Marolleau, J.P., Seymour, B., Larghero, J., Lake, S., Chatellier, G., Solomon, S., Desnos, M., and Hagège, A.A. The myoblast autologous grafting in ischemic cardiomyopathy (MAGIC) trial first randomized Placebo-controlled study of myoblast transplantation. Circulation **117,** 1189, 2008.
16. Wagers, A.J., Sherwood, R.I., Christensen, J.L., and Weissman, I.L. Little evidence for developmental plasticity of adult hematopoietic stem cells. Science **297,** 2256, 2002.
17. Chien, K.R. Stem cells: lost in translation. Nature **428,** 607, 2004.
18. Muller-Ehmsen, J., Whittaker, P., Klonar, R.A., Dow, J.S., Sakoda, T., Long, T.I., Laird, P.W., and Kedes, L. Survival

and development of neonatal rat cardiomyocytes transplanted into adult myocardium. J Mol Cell Cardiol **34,** 107, 2002.
19. Leor, J., Amsalem, Y., and Cohen, S. Cells, scaffolds, and molecules for myocardial tissue engineering. Pharmacol Ther **105,** 151, 2005.
20. Dvir, T., Kedem, A., Ruvinov, E., Levy, O., Freeman, I., Landa, N., Holbova, R., Feinburg, M.S., Dror, S., Etzion, Y., Leor, J., and Cohen, S. Prevascularization of cardiac patch on the omentum improves its therapeutic outcome. Proc Natl Acad Sci USA **106,** 16568, 2009.
21. Stevens, K., Pabon, L., Muskheil, V., and Murry, C. Scaffold-free human cardiac tissue patch created from embryonic stem cells. Tissue Eng Part A **15,** 1211, 2009.
22. Thai, H., Juneman, E., Lancaster, J., Hagerty, T., Do, R., Castellano, L., Kellar, R., Williams, S., Sethi, G., Schmelz, M., Gaballa, M.A., and Goldman, S. Implantation of a 3-dimensional fibroblast matrix improves left ventricular function and blood flow after acute myocardial infarction. Cell Transplant **18,** 283, 2009.
23. Aoki, M., Morishita, R., Taniyama, Y., Kida, I., Moriguchi, A., Matsumoto, K., Nakamura, T., Kaneda, Y., Higaki, J., and Ogihara, T. Angiogenesis induced by heptocyte growth factor in non-infarcted myocardium and infarcted myocardium: up regulation of essential transpcription factor for angiogenesis. Gene Ther **7,** 417, 2000.
24. Melillo, G., Lima, J.A.C., Judd, R.M., Goldschmidt-Clermont, P.J., and Silverman, H.S. Intrinsic myocyte dysfunction and tyrosine kinase pathway activation underlie the impaired wall thickening of adjacent regions during postinfarct left ventricular remodeling. Circulation **93,** 1447, 1996.
25. Yang, Y., Min, J.Y., Rana, J.S., Ke, Q., Cai, J., Chen, Y., Morgan, J.P., and Xiao, Y.F. VEGF enhances functional improvement of postinfarcted hearts by transplantation of ESC-differentiated cells. J Appl Physiol **93,** 1140, 2002.
26. Gaballa, M.A., Raya, T.E., and Goldman, S. Large artery remodeling after myocardial infarction. Am J Physiol **268,** H2092, 1995.
27. Goldman, S., and Raya, T.E. Rat infarct model of myocardial infarction and heart failure. J Card Fail **1,** 169, 1995.
28. Gaballa, M.A., and Goldman, S. Ventricular remodeling in heart failure. J Card Fail **6,** S476, 2002.
29. Pennock, G.D., Raya, T.E., Bahl, J.J., Goldman, S., Morkin E. Combination treatment with captopril and the thyroid hormone analog 3,5 diiodothyroproprionic acid (DITPA): a new approach to improving left ventricular performance in heart failure. Circulation **88,** 1289, 1993.
30. Raya, T.E., Gay, R.G., Aguirre, M., and Goldman, S. The importance of venodilatation in the prevention of left ventricular dilatation after chronic large myocardial infarction in rats: a comparison of captopril and hydralazine. Circ Res **64,** 330, 1989.
31. Raya, T.E., Gaballa, M., Anderson, P., and Goldman, S. Left ventricular function and remodeling after myocardial infarction in aging rats. Am J Physiol **273(6 Pt 2),** H2652,1997.
32. Thai, H., Castellano, L., Juneman, E., Phan, H., Do, R., Gaballa, M.A., and Goldman, S. Pretreatment with angiotensin receptor blockade prevents left ventricular dysfunction and blunts LV remodeling associated with acute myocardial infarction. Circulation **114,** 1933, 2006.
33. Kellar, R.S., Landeen, L.K., Shephred, B.R., *et al.* Scaffold-Based 3-D Human fibroblast culture provides a structural matrix that support angiogenesis in infarcted heart tissue. Circulation **104,** 2063, 2001.
34. Kellar, R.S., Shepherd, B.R., Larson, D.F., Naughton, G.K., and Williams, S.K. A cardiac patch constructed from human fibroblasts attenuates a reduction in cardiac function following acute infarct. Tissue Eng **11/12,** 1678, 2005.
35. Kern, A., Liu, K., and Mansbridge, J. Modification of fibroblast gamma-interferon responses by extracellular matrix. Invest Dermatol **17,** 112, 2001.
36. Gaballa, M.A., Sunkomat, J.N.E., Morkin, E., Ewy, G., and Goldman, S. Grafting an acellular 3-D collagen scaffold onto a non-transmural cryoinjured myocardium induces neoangiogenesis and retards cardiac remodeling. J Heart Lung Transplant **25,** 946, 2006.
37. Fukuda, S., Kaga, S., Sasaki, H., Zhan, L., Zhu, L., Otani, H., Kalfin, R., Das, D.K., and Maulik, N. Angiogenic signal triggered by ischemic stress induces myocardial repair in rat during chronic infarction. J Mol Cell Cardiol **36,** 547, 2004.
38. Lei, L., Zhou, R., Zheng, W., Christensen, L., Weiss, R., and Tomanek, R. Bradycardia induces angiogenesis, increases coronary reserve, and preserves function of the postinfarcted heart. Circulation **17,** 796, 2004.
39. Reinhardt, C.P., Dalberg, S., Tries, M.A., Marcel, R., and Leppo, J.A. Stable labeled microspheres to measure perfusion: validation of a neutron activation assay technique. Am J Physiol **280,** H108, 2001.
40. Hahn, J.Y., Cho, H.J., Kang, H.J., Kim, T.S., Kim, M.H., Chung, J.H., Bae, J.W., Oh, B.H., Park, Y.B., and Kim, H.S. Pre-treatment of mesenchymal stem cells with a combination of growth factors enhances gap junction formation, cytoprotective effect on cardiomyocytes, and therapeutic efficacy for myocardial infarction. J Am Coll Cardiol **51,** 933, 2008.
41. Ma, J., Wang, Q., Fei, T., Han, J., and Chen, Y.G. MCP-1 mediates TGF-B-induced angiogenesis by stimulating vascular smooth muscle cell migration. Blood **1,** 987, 2007.
42. Li, A., Dubey, S., Varney, M.L., Dave, B.J., and Singh, R.K. IL-8 directly enhanced endothelial cell survival, proliferation, and matrix metalloproteinases production and regulated angiogenesis. J Immunol **15,** 3369, 2003.
43. Shirmer, S., Buschmann, I.R., Jost, M.M., Hoefer, I.E., Grundman, S., Andert, J.-P., Ulusans, S., Bode, C., Piek, J.J., and van Royen, N. Differential effects of MCP-1 and leptin on collateral flow and angiogenesis. Cardiovasc Res **64,** 356, 2004.
44. Webb, K., Hitchcock, R., Smeal, S., Li, W., Gray, S., and Tresco, P. Cyclic strain increases fibroblast proliferation, matrix accumulation, and elastic modulus of fibroblast-seeded polyurethane constructs. J Biomech **39,** 1136, 2004.
45. Dow, J., Simkhovich, B.Z., Kedes, L., and Klonar, R.A. Wash-out of transplanted cells from the heart: a potential new hurdle for cell transplantation therapy. Cardiovasc Res **67,** 301, 2005.

Address correspondence to:
Jordan J. Lancaster, B.S.
3601 S. 6th Ave.
Southern Arizona VA Health Care System
Cardiology 1-111C
Tucson, AZ 85723

E-mail: Jordan.Lancaster@VA.gov

Received: September 2, 2009
Accepted: May 11, 2010
Online Publication Date: July 28, 2010

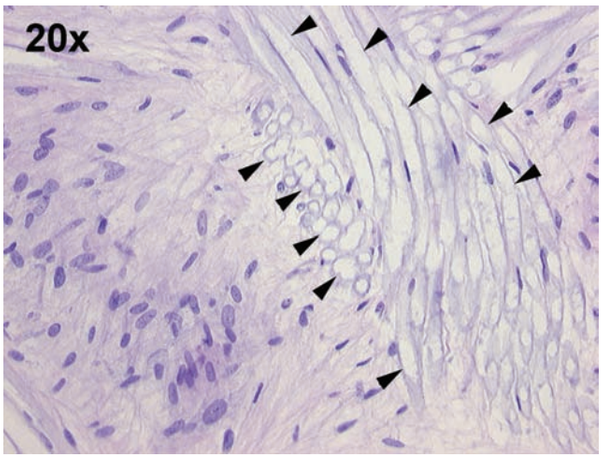

SUPPLEMENTAL FIG. S1. Hematoxylin and eosin stain of the three-dimensional fibroblast construct (3DFC) at 20 min after thawing from −75°C. Arrowheads denote vicryl mesh construct of the 3DFC that provide structure and support for resident fibroblast growth and proliferation.

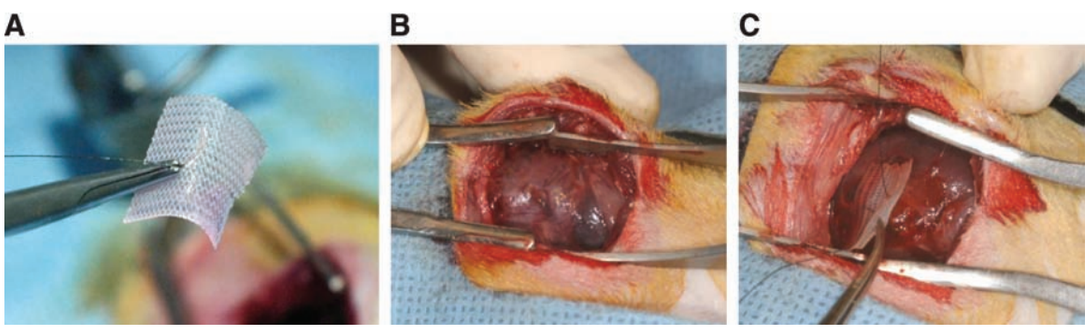

SUPPLEMENTAL FIG. S2. The 3DFC before implantation (**A**), chest open with a infarcted dilated heart 3 weeks after coronary artery ligation (**B**), and 3DFC placed on this dilated infarcted heart (**C**).

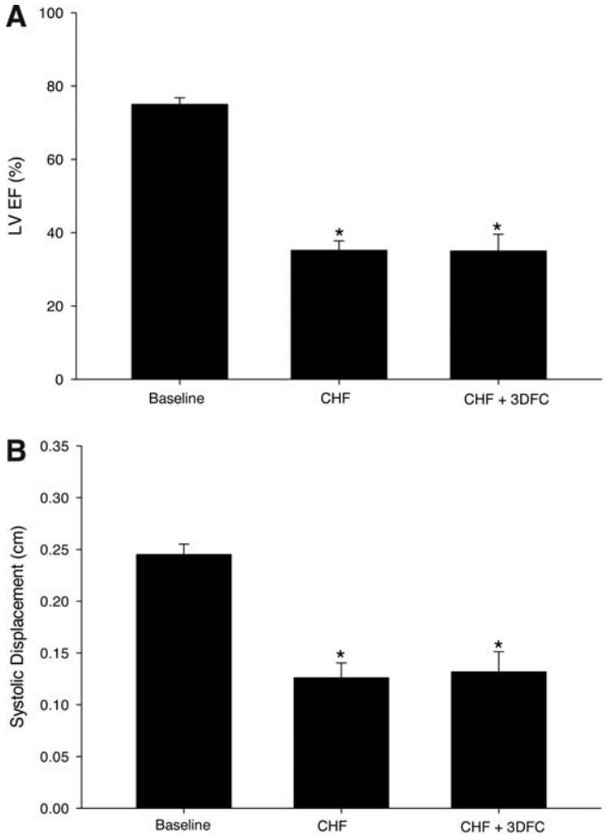

SUPPLEMENTAL FIG. S3. (**A**) Ejection fraction (EF) in chronic heart failure (CHF) after 3DFC. Values are mean ± standard error (SE); sham, $n = 10$; CHF, $n = 6$; CHF 3DFC, $n = 6$. *$p < 0.05$ versus sham. (**B**) Systolic displacement of the infarcted wall in CHF with 3DFC. Values are mean ± SE; sham, $n = 10$; CHF, $n = 6$; CHF+3DFC, $n = 6$. *$p < 0.05$ versus sham.

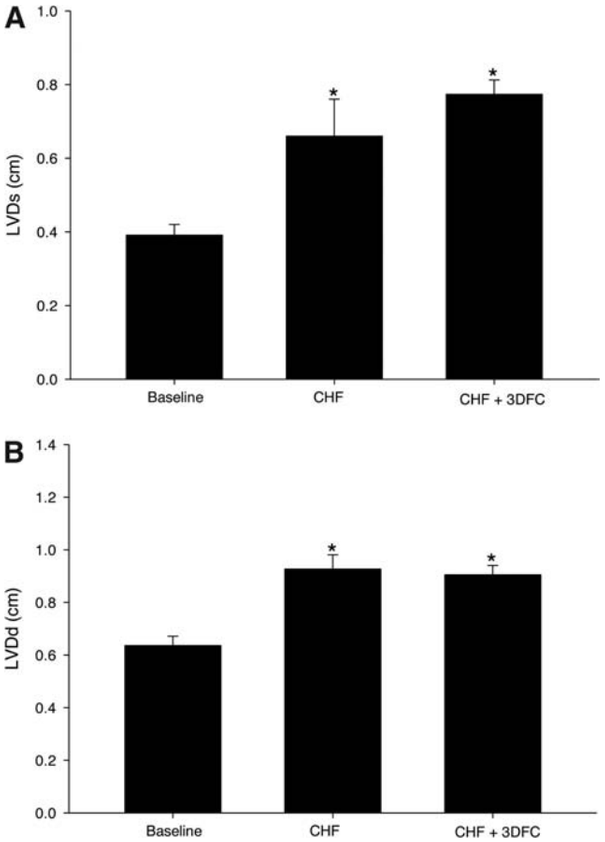

SUPPLEMENTAL FIG. S4. (**A**) Left ventricular (LV) end systolic diameter (LVDs) with 3DFC in CHF. Values are mean ± SE; sham, $n = 10$; CHF, $n = 6$; CHF+3DFC, $n = 6$. *$p < 0.05$ versus sham. (**B**) LV end-diastolic diameter (LVDd) with 3DFC in CHF. Values are mean ± SE; sham, $n = 10$; CHF, $n = 6$; CHF + 3DFC, $n = 6$. *$p < 0.05$ versus sham.

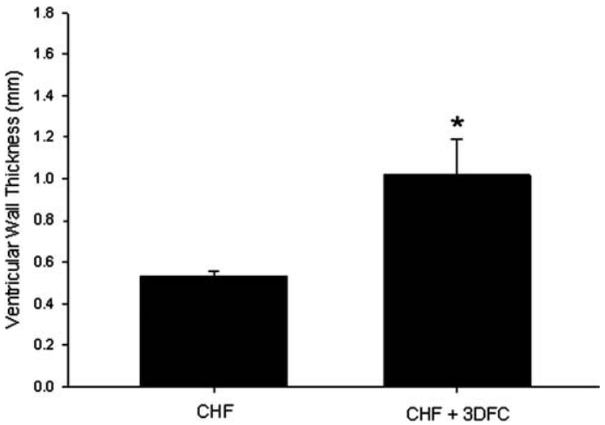

SUPPLEMENTAL FIG. S5. Ventricular wall thickness in rats with CHF versus 3DFC-treated hearts. Implantation of the 3DFC in rats with CHF increases LV wall thickness. *Statistical significance ($p < 0.05$). Values are mean + SE; CHF, $n = 5$; CHF+3DF, $n = 5$.